

Synthesis of Wideband Cross-Coupled Resonator Filter for Direct Circuit Implementation Using Lumped Elements

Bin Liu¹, Graduate Student Member, IEEE, Kun Li, Xiong Chen, Pei-Ling Chi², Senior Member, IEEE, and Tao Yang¹, Senior Member, IEEE

Abstract—A synthesis method of wideband cross-coupled resonator filter with inductive and capacitive coupling components is presented using similarity transformation. The synthesized admittance matrix can fully represent the frequency-dependent characteristics of the J -inverters that are used to implement the coupling components. All negative inductive-coupling elements obtained from the conventional wideband filter synthesis method can be transformed to positive capacitive coupling elements by solving the equation derived from similarity transformation, so that the resulted admittance matrix can be directly implemented using lumped elements. All values of the lumped elements can be calculated without any optimization. A third-order triplet with fractional bandwidth (FBW) of 50% and one transmission zero (TZ) in the lower stopband and a fourth-order quadruplet with FBW of 50% and two symmetrical TZs are synthesized to demonstrate the proposed method.

Index Terms—Admittance matrix, lumped element, similarity transformation, synthesis method, wideband bandpass filter (BPF).

I. INTRODUCTION

WIDEBAND bandpass filter (BPF) is an essential component in wideband receiver systems [1], [2]. Numerous wideband BPFs using different topologies and design methods have been proposed in past years [3], [4], [5], [6], [7], [8], [9], [10], [11]. Due to the reason that the constant coupling coefficient in a coupling matrix is met only at the center frequency during circuit implementation, the classic matrix synthesis method proposed in [12] and [13] are, all most effective for narrowband filters. The frequency-dependent coupling (FDC) in the synthesized coupling matrix in [14], [15], [16], and [17] can be implemented by parallel connected π -networks of capacitors and inductors, however, these methods are also only effective for narrowband filters.

To synthesize wideband BPF with a given filter specification, many new synthesis methods have been proposed in the past years [3], [4], [5], [18]. In [18], a synthesis method for

Manuscript received 21 February 2023; accepted 1 April 2023. This work was supported in part by the Sichuan Province Engineering Research Center for Broadband Microwave Circuit High Density Integration and in part by the National Natural Science Foundation of China under Grant 62171105 and Grant 62271110. (Corresponding author: Tao Yang.)

Bin Liu, Kun Li, Xiong Chen, and Tao Yang are with the School of Electronic Science and Engineering, University of Electronic Science and Technology of China, Chengdu, Sichuan 610054, China (e-mail: yangtao8314@uestc.edu.cn).

Pei-Ling Chi is with the Department of Electrical and Computer Engineering, National Chiao Tung University, Hsinchu 300, Taiwan.

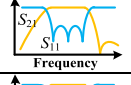
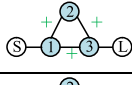
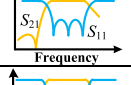
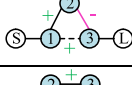
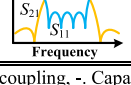
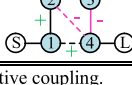
This article was presented at the IEEE MTT-S International Microwave Symposium (IMS 2023), San Diego, CA, USA, June 11–16, 2023.

Color versions of one or more figures in this letter are available at <https://doi.org/10.1109/LMWT.2023.3266274>.

Digital Object Identifier 10.1109/LMWT.2023.3266274

TABLE I

RELATIONSHIP BETWEEN FILTER RESPONSE, TOPOLOGY, AND NEEDED FDC

Case	TZ	Response	Topology	Needed FDC
I	One right TZ			$\frac{1}{\omega L}$
II	One left TZ			$\frac{1}{\omega L}, -\frac{1}{\omega L}$
III	Two symmetrical TZs			$\frac{1}{\omega L}, -\frac{1}{\omega L}$

+, Defined as inductive coupling, -, Capacitive coupling.

lumped element BPF is proposed on the basis of the FDC matrix. This method is, however, only effective for filters with moderate fractional bandwidth (FBW). In [3], polynomial and coupling matrices for wideband BPF are synthesized directly in the bandpass domain with inductive FDC. This method is applicable to filters with arbitrary bandwidth, however, the FDC in this method is only limited to either positive or negative inductive FDC. There still remains a challenge that the resulting coupling matrix may be physically unrealizable when both negative and positive FDC components exist in the synthesized coupling matrix.

Table I shows the classic topologies to implement the wideband BPF with different transmission zero (TZ) locations at the lower stopband, upper stopband, or two sides of the filter passband. For a third-order BPF with one TZ at the upper stopband (Case I in Table I), only positive inductive FDC $1/(\omega L)$ is needed [3], and the FDC of $1/(\omega L)$ represents the J -inverter with a value of $1/(\omega L)$ which can be theoretically realized using a π -type inductor network [19]. However, when there is a TZ located at the lower stopband as Case II and Case III in Table I, inductive FDC of $-1/(\omega L)$ exists in the coupling matrix which has a negative sign. This FDC of $-1/(\omega L)$ represents a J -inverter with a value of $-1/(\omega L)$ which cannot be directly implemented with practical lumped elements. Similar challenges exist for higher-order filters as well. Due to these physically unrealizable coupling, the synthesized BPF cannot be physically implemented using lumped elements.

In this letter, a lumped element synthesis method for cross-coupled wideband BPF with inductive and capacitive FDC is proposed for the first time. The negative FDC of $-1/(\omega L)$ can be transformed into a positive capacitive FDC of $-\omega C$. Note that the FDC of $-\omega C$ represents a J -inverter with a value of $J = \omega C$, and can be realized by π -type capacitor network [19]. With this transformation, the synthesized admittance matrix for the wideband filter can be directly implemented using lumped elements.

II. SYNTHESIS OF THE THIRD-ORDER AND FOURTH-ORDER BPF

A. Synthesis of Third-Order BPF With One TZ at the Lower Stopband

To synthesize a wideband BPF with TZ at the lower stopband as the Case II in Table I, the synthesis process begins with the synthesized folded admittance matrix expressed as (1) using the synthesis method proposed in [3]

$$A_1 = \begin{array}{ccccc|c} \text{S} & \text{1} & \text{2} & \text{3} & \text{L} & \\ \hline -j & M'_{S1} & 0 & 0 & 0 & \text{S} \\ M'_{S1} & M_{11} & M_{12} & M_{13} & 0 & \text{1} \\ 0 & M_{12} & M_{22} & M_{23} & 0 & \text{2} \\ 0 & M_{13} & M_{23} & M_{33} & M'_{3L} & \text{3} \\ 0 & 0 & 0 & M'_{3L} & -j & \text{L} \end{array} \quad (1)$$

where M_{ii} ($i = 1, 2, 3$) is the self-coupling of resonator i and M_{ij} ($i, j = 1, 2, 3, i \neq j$) represent the coupling between resonator i and resonator j . It has

$$\begin{aligned} M_{ii} &= \omega C'_i - \omega_i'^2/\omega, & M_{12} &= 1/\omega L'_{12}, \\ M_{23} &= 1/\omega L'_{23}, & M_{13} &= -1/\omega L'_{13} \end{aligned} \quad (2)$$

where $C'_i = 1 \text{ F}$ ($i = 1, 2, 3$) and $\omega_i'^2 = 1/L'_i$ which is the resonant frequency of the i th resonator. C'_i and L'_i are capacitance and inductance of the parallel resonators, L'_{ij} is the needed coupling inductance in the actual circuit and it has $L'_{12} = L'_{23}$. Investigating the matrix in (1), the FDC of $1/(\omega L'_{12})$ and $1/(\omega L'_{23})$ for M_{12} and M_{23} can be represented and implemented using inductive lumped J -inverters with the value of $1/(\omega L'_{12})$ and $1/(\omega L'_{23})$ [19]. However, the component of $-1/(\omega L'_{13})$ for M_{13} cannot be implemented using any physical inductive or capacitive lumped J -inverter. To implement this negative FDC, the negative inductive coupling $-1/(\omega L'_{13})$ need to be transformed into a positive inductive coupling $1/(\omega L'_{13})$ or capacitive coupling $-\omega C'_{13}$ ($J = \omega C'_{13}$). To solve this problem, a similarity transformation is performed to (1) by $A_2 = TA_1T^T$, where the orthogonal matrix T is defined as

$$T = \begin{bmatrix} 1 & 0 & 0 & 0 & 0 \\ 0 & 1 & 0 & 0 & 0 \\ 0 & 0 & 1 & Pm & 0 \\ 0 & 0 & 0 & c_1 & 0 \\ 0 & 0 & 0 & 0 & 1 \end{bmatrix} \quad (3)$$

where Pm and c_1 are two real variables. The resulting new matrix A_2 can be obtained as

$$A_2 = \begin{bmatrix} -j & M'_{S1} & 0 & 0 & 0 \\ M'_{S1} & \omega - \frac{\omega_1'^2}{\omega} & \frac{1}{\omega L'_{12}} & \frac{k_{13}}{\omega} & 0 \\ 0 & \frac{1}{\omega L'_{12}} & \omega - \frac{\omega_2'^2}{\omega} & Pm \cdot \omega + \frac{k_1}{\omega} & 0 \\ 0 & \frac{k_{13}}{\omega} & Pm \cdot \omega + \frac{k_1}{\omega} & k_2\omega + \frac{k_3}{\omega} & c_1 M'_{3L} \\ 0 & 0 & 0 & c_1 M'_{3L} & -j \end{bmatrix} \quad (4)$$

where

$$\begin{aligned} k_1 &= c_1/L'_{23} - Pm \cdot \omega_2'^2, & k_{13} &= Pm/L'_{23} - c_1/L'_{13} \\ k_2 &= Pm^2 + c_1^2, & k_3 &= 2c_1 Pm/L'_{23} - Pm^2 \omega_2'^2 - c_1^2 \omega_3'^2. \end{aligned}$$

Investigating (4), in order to make the coupling M_{23} in (4) simple and physically realizable, the coefficient for $1/\omega$ of M_{23} in (4) needs to be 0, while the coefficient of $1/\omega$ of M_{13}

in (4) needs to be larger than 0. This leads to the conditions as

$$-Pm \cdot \omega_2'^2 + c_1/L'_{23} = 0 \quad (5)$$

$$Pm/L'_{12} - c_1/L'_{13} > 0. \quad (6)$$

Once (5) and (6) are satisfied, the couplings in the resulting matrix are all pure inductive couplings and pure capacitive couplings. The value of Pm is solved by (5) and c_1 can be arbitrarily chosen to satisfy (6), and it has

$$Pm = c_1/(\omega_2'^2 L'_{23}). \quad (7)$$

As a result, the new admittance matrix A_2 in (4) has

$$\begin{aligned} k_1 &= 0, & k_{13} &= c_1/(\omega_2'^2 L'_{12}) - c_1/L'_{13} \\ k_2 &= c_1^2/(\omega_2'^4 L'_{12}) + c_1^2, & k_3 &= 1/(\omega_2'^2 L'_{12}) - \omega_3'^2. \end{aligned} \quad (8)$$

From (4), (7) and (8), it can be found that all the inductive coupling components are positive while the capacitive coupling components are negative, so they can be now practically implemented using lumped elements.

To further reduce the circuit complexity, the external coupling of M'_{S1} and M'_{3L} in the coupling matrix can be scaled to 1 by performing a similarity transformation of $A_3 = T_s A_2 T_s^T$ [10], where T_s is a scaling matrix defined as

$$T_s = \text{diag}\left(1, 1/M'_{S1}, \sqrt{C_2}, |1/(c_1 M'_{3L})|, 1\right) \quad (9)$$

and C_2 is the specified capacitance of the second resonator. The resulting admittance matrix can be expressed as

$$A_3 = \begin{bmatrix} -j & 1 & 0 & 0 & 0 \\ 1 & \omega C_1 - \frac{1}{\omega L_1} & \frac{1}{\omega L_{12}} & \frac{1}{\omega L_{13}} & 0 \\ 0 & \frac{1}{\omega L_{12}} & \omega C_2 - \frac{1}{\omega L_2} & -\omega C_{23} & 0 \\ 0 & \frac{1}{\omega L_{13}} & -\omega C_{23} & \omega C_3 - \frac{1}{\omega L_3} & -1 \\ 0 & 0 & 0 & -1 & -j \end{bmatrix} \quad (10)$$

where the capacitance and inductance can be calculated as

$$\begin{aligned} C_1 &= \frac{1}{M_{S1}^2}, & C_3 &= \frac{1 + \omega_2'^4 L_{12}^2}{\omega_2'^4 L_{12}^2 M_{S1}^2}, & L_{12} &= \frac{M'_{S1} L'_{12}}{\sqrt{C_2}} \\ L_1 &= \frac{M_{S1}^2}{\omega_1'^2}, & L_2 &= \frac{1}{\omega_2'^2 C_2}, & L_3 &= \frac{M_{S1}^2 \omega_2'^2 L_{23}^2}{(1 - \omega_2'^2 L_{23}^2 \omega_3'^2)} \\ L_{13} &= \frac{M_{S1}^2 |c_1| \omega_2'^2 L_{12}^2 L'_{13}}{c_1 (L'_{13} - \omega_2'^2 L_{12}^2)}, & C_{23} &= \frac{c_1 \sqrt{C_2}}{\omega_2'^2 L'_{12} M'_{S1} |c_1|}. \end{aligned} \quad (11)$$

With the admittance matrix in (10), the circuit schematic of the proposed wideband BPF can be directly implemented and is shown in Fig. 1(a) [19], [20]. The resonator 1 and 3 are connected to the source and load directly, respectively, since M'_{S1} and M'_{3L} have been transformed to 1 or -1 in (10), which significantly reduces the circuit complexity.

As a numerical example, a third-order wideband BPF with f_L at 0.9 GHz, f_H at 1.5 GHz (where f_L and f_H are the lower and upper cut-off frequencies of the passband, respectively), one TZ at 0.6 GHz, and return loss of 20 dB is synthesized following the proposed procedure. The final synthesized element values are given in Table II according to the calculated parameters in (11). Note that the values in Table II are normalized at the input and output impedance of 1 Ω . With the coupling matrix in (10) and components

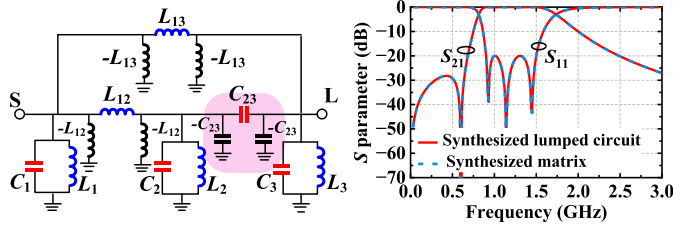


Fig. 1. (a) Circuit of synthesized third-order wideband BPF with one capacitive coupling. (b) Comparison between responses of synthesized matrix and the synthesized corresponding circuit of (a).

values from Table II, the physical circuit can be then directly implemented using lumped elements as given in Fig. 1(a). The negative components of the J -inverters in Fig. 1(a) can be absorbed by adjacent resonators. The responses of the synthesized matrix and the simulated results of the lumped element circuit are shown in Fig. 1(b). Both results agree excellently with each other, validating the advance of the synthesized matrix using the proposed method.

B. Synthesis of Fourth Order Wideband BPF With Two TZs

Similarly, the proposed method can be applied to higher-order filters. For demonstration purposes, a fourth-order wideband BPF with two symmetry TZs in the upper and lower stopband as Case III in Table I is synthesized here. First, the initial matrix can be synthesized using the classic synthesized method for wideband filter [3] as

$$B_1 = \begin{bmatrix} -j & M'_{S1} & 0 & 0 & 0 & 0 \\ M'_{S1} & \omega - \frac{\omega_1^2}{\omega} & \frac{1}{\omega L'_{12}} & 0 & -\frac{1}{\omega L'_{14}} & 0 \\ 0 & \frac{1}{\omega L'_{12}} & \omega - \frac{\omega_2^2}{\omega} & \frac{1}{\omega L'_{23}} & -\frac{1}{\omega L'_{24}} & 0 \\ 0 & 0 & \frac{1}{\omega L'_{23}} & \omega - \frac{\omega_3^2}{\omega} & \frac{1}{\omega L'_{34}} & 0 \\ 0 & -\frac{1}{\omega L'_{14}} & -\frac{1}{\omega L'_{24}} & \frac{1}{\omega L'_{34}} & \omega - \frac{\omega_4^2}{\omega} & M'_{4L} \\ 0 & 0 & 0 & 0 & M'_{4L} & -j \end{bmatrix}. \quad (12)$$

As previously discussed, the negative coupling component of $-1/(\omega L'_{14})$ and $-1/(\omega L'_{24})$ cannot be directly implemented using lumped elements. In order to get the matrix without negative inductive coupling, the similarity transformation process similar to Section II-A can be applied. The similarity transformation of $B_2 = TB_1T^T$ can be used, where the orthogonal matrix T is defined as

$$T = \begin{bmatrix} 1 & 0 & 0 & 0 & 0 & 0 \\ 0 & 1 & 0 & 0 & 0 & 0 \\ 0 & 0 & 1 & 0 & Pg & 0 \\ 0 & 0 & 0 & 1 & Pn & 0 \\ 0 & 0 & 0 & 0 & c_1 & 0 \\ 0 & 0 & 0 & 0 & 0 & 1 \end{bmatrix}. \quad (13)$$

To eliminate the negative inductive coupling component, the following conditions need to be satisfied:

$$-Pg \cdot \omega_2^2 + Pn/L'_{23} - c_1/L'_{24} = 0 \quad (14)$$

$$-Pn \cdot \omega_3^2 + Pg/L'_{23} + c_1/L'_{34} = 0 \quad (15)$$

$$Pg/L'_{12} - c_1/L'_{14} > 0. \quad (16)$$

TABLE II
ELEMENT VALUE OF SYNTHESIZED MATRIX OF CONFIGURATION (10)

Element	C_1 (pF)	C_2 (pF)	C_3 (pF)	L_1 (nH)	L_2 (nH)	L_3 (nH)	L_{12} (nH)	L_{13} (nH)	C_{23} (pF)
Value	226.3	250	295.4	0.063	0.084	0.08	0.16	0.72	131

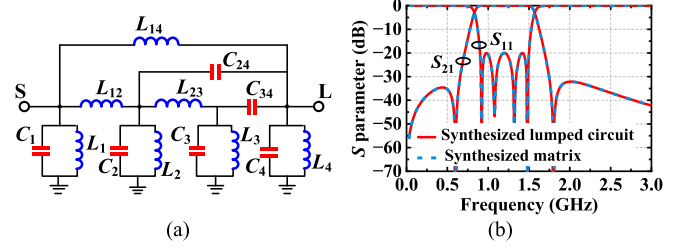


Fig. 2. (a) Schematic of fourth-order filter (all negative elements have been absorbed to the adjacent resonators, $C_1 = 5$ pF, $C_2 = 4.5$ pF, $C_3 = 2.68$ pF, $C_4 = 3.4$ pF, $L_1 = 5.49$ nH, $L_2 = 11$ nH, $L_3 = 5.49$ nH, $L_4 = 3.96$ nH, $L_{12} = 7.95$ nH, $L_{23} = 9.26$ nH, $C_{34} = 2.3$ pF, $L_{14} = 69.8$ nH, $C_{24} = 0.46$ pF. And the input and output impedance are de-normalized to 50 Ω). (b) Comparison between the response of synthesized matrix and the synthesized circuit of (a).

The value of p_n and P_g can be solved by (14) and (15) as

$$Pg = \frac{L'_{23}c_1(L'_{23}L'_{34}\omega_3^2 - L'_{24})}{L'_{34}L'_{24}(1 - \omega_2^2\omega_3^2L'_{23})}$$

$$Pn = \frac{L'_{23}c_1(L'_{23}L'_{24}\omega_3^2 - L'_{34})}{L'_{34}L'_{24}(1 - \omega_2^2\omega_3^2L'_{23})}. \quad (17)$$

After scaling the external coupling of M'_{S1} and M'_{4L} , the final admittance matrix can be obtained as

$$B_3 = \begin{bmatrix} -j & 1 & 0 & 0 & 0 & 0 \\ 1 & \omega C_1 - \frac{1}{\omega L_1} & \frac{1}{\omega L_{12}} & 0 & \frac{1}{\omega L_{14}} & 0 \\ 0 & \frac{1}{\omega L_{12}} & \omega C_2 - \frac{1}{\omega L_2} & \frac{1}{\omega L_{23}} & -\omega C_{24} & 0 \\ 0 & 0 & \frac{1}{\omega L_{23}} & \omega C_3 - \frac{1}{\omega L_3} & -\omega C_{34} & 0 \\ 0 & \frac{1}{\omega L_{14}} & -\omega C_{24} & -\omega C_{34} & \omega C_4 - \frac{1}{\omega L_4} & 1 \\ 0 & 0 & 0 & 0 & 1 & -j \end{bmatrix} \quad (18)$$

where

$$C_1 = \frac{1}{M_{S1}^2}, \quad L_1 = \frac{M_{S1}^2}{\omega_1^2}, \quad L_2 = \frac{1}{\omega_2^2 C_2}, \quad C_{24} = \frac{Pg\sqrt{C_2}}{M_{S1}|c_1|}$$

$$L_3 = \frac{1}{\omega_3^2 C_3}, \quad C_4 = \frac{(Pg^2 + Pn^2 + c_1^2)}{M_{S1}^2|c_1|^2}, \quad C_{34} = \frac{Pn\sqrt{C_3}}{M_{S1}|c_1|}$$

$$L_{12} = \frac{M_{S1}L'_{12}}{\sqrt{C_2}}, \quad L_{23} = \frac{L'_{23}}{\sqrt{C_2}\sqrt{C_3}}, \quad L_{14} = \frac{L'_{12}L'_{14}M_{S1}^2|c_1|}{PgL'_{14} - c_1L'_{12}}$$

$$L_4 = M_{S1}^2|c_1|^2 \left(\frac{1}{\omega_4^2 c_1^2} - \frac{L'_{24}}{c_1 Pg} - \frac{L'_{34}}{c_1 Pn} \right). \quad (19)$$

From (18) and (19), it can be found that all the negative inductive couplings have been eliminated and the matrix can be directly implemented using the lumped circuit.

As an example, a fourth-order wideband BPF with $f_L = 0.9$ GHz, $f_H = 1.5$ GHz, two TZs at 0.6 and 1.8 GHz, and a return loss of 20 dB is synthesized using the proposed procedure. Fig. 2(a) shows the implemented circuit using lumped components according to the matrix (18). Note that all negative inductors and capacitors in J -inverters have been absorbed by the adjacent lumped elements. Assuming that $c_1 = -1$,

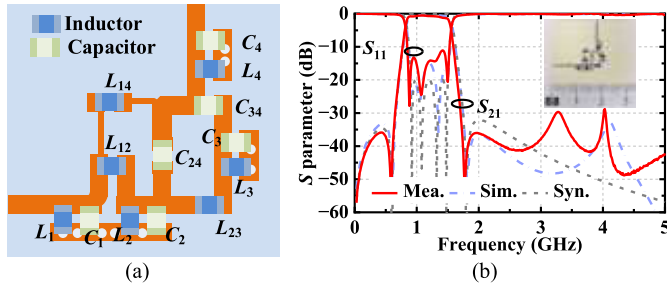


Fig. 3. (a) Layout of the validation circuit of synthesized fourth-order wideband BPF. (b) Measured, simulated, and synthesized S -parameters for fabricated filter.

the final synthesized element values after de-normalization to $50\ \Omega$ and absorbing of negative elements are given in the caption of Fig. 2. The response of the synthesized matrix and the simulated results of lumped element circuit in Fig. 2(a) are shown in Fig. 2(b). We can see that lumped circuit response using synthesized values align well with the synthesized matrix response at the full frequency domain which further certifies the advance of the proposed synthesis method of the lumped circuit for wideband BPF.

III. VALIDATION AND MEASUREMENTS

To validate the proposed synthesis method, the circuit of the schematic in Fig. 2(a) is fabricated on a single-layer substrate of Rogers4350B with $\epsilon_r = 3.66$ and thickness $h = 0.508$ mm. Fig. 3(a) shows the layout of the designed circuit and the placement position of the lumped elements. The photograph of the fabricated wideband BPF is given in Fig. 3(b). Hollow 0603 HP inductors are used as the fixed inductors and ATC600s capacitors are used as the fixed capacitors.

Fig. 3(b) shows the comparison of the measured, EM simulated, and synthesized S -parameters for the fabricated circuit. As can be found, all results agree reasonably well with each other, validating the proposed method. The measured filter passband is from 0.85 to 1.53 GHz with an FBW of 57.1%. The measured return loss in the passband is better than 11 dB and the minimum insertion loss is 0.54 dB. TZs at 0.59 and 1.77 GHz are observed on both sides of the passband.

IV. CONCLUSION

In this letter, a matrix synthesis method for third-order and fourth-order wideband BPF is proposed for direct circuit implementation using lumped elements. Using the proposed method, the elements in the synthesized coupling matrix can correspond to the values of capacitance and inductance in the actual circuit without any optimization, which simplifies the design process of wideband lumped element filters. The detail synthesis method for a third-order filter with one left TZ and a fourth-order filter with two TZs at each side of the passband are given. Furthermore, a fourth-order filter with FBW of 50% is designed and fabricated according to the synthesized element value to demonstrate the proposed method.

REFERENCES

- [1] M. Ranjan and L. E. Larson, "A low-cost and low-power CMOS receiver front-end for MB-OFDM ultra-wideband systems," *IEEE J. Solid-State Circuits*, vol. 42, no. 3, pp. 592–601, Mar. 2007.
- [2] F. S. Lee and A. P. Chandrakasan, "A BiCMOS ultra-wideband 3.1–10.6-GHz front-end," *IEEE J. Solid-State Circuits*, vol. 41, no. 8, pp. 1784–1791, Aug. 2006.
- [3] S. Amari, F. Seyfert, and M. Bekheit, "Theory of coupled resonator microwave bandpass filters of arbitrary bandwidth," *IEEE Trans. Microw. Theory Techn.*, vol. 58, no. 8, pp. 2188–2203, Aug. 2010.
- [4] W. Meng, H.-M. Lee, K. A. Zaki, and A. E. Atia, "Synthesis of wideband multicoupled resonators filters," *IEEE Trans. Microw. Theory Techn.*, vol. 59, no. 3, pp. 593–603, Mar. 2011.
- [5] R. Zhang, S. Luo, and L. Zhu, "A new synthesis and design method for wideband bandpass filters with generalized unit elements," *IEEE Trans. Microw. Theory Techn.*, vol. 65, no. 3, pp. 815–823, Mar. 2017.
- [6] L. Zhu, S. Sun, and W. Menzel, "Ultra-wideband (UWB) bandpass filters using multiple-mode resonator," *IEEE Microw. Wireless Compon. Lett.*, vol. 15, no. 11, pp. 796–798, Nov. 2005.
- [7] Z. C. Hao and J. S. Hong, "Ultra-wideband bandpass filter using multilayer liquid-crystal-polymer technology," *IEEE Trans. Microw. Theory Techn.*, vol. 56, no. 9, pp. 2095–2100, Sep. 2008.
- [8] B. Zhang, Y. Wu, and Y. Liu, "Wideband single-ended and differential bandpass filters based on terminated coupled line structures," *IEEE Trans. Microw. Theory Techn.*, vol. 65, no. 3, pp. 761–774, Mar. 2017.
- [9] S. Arain, P. Vryonides, M. A. B. Abbasi, A. Qudus, M. A. Antoniadis, and S. Nikolaou, "Reconfigurable bandwidth bandpass filter with enhanced out-of-band rejection using π -section-loaded ring resonator," *IEEE Microw. Wireless Compon. Lett.*, vol. 28, no. 1, pp. 28–30, Jan. 2018.
- [10] F. Mira, J. Mateu, S. Cogollos, and V. E. Boria, "Design of ultra-wideband substrate integrated waveguide (SIW) filters in zigzag topology," *IEEE Microw. Wireless Compon. Lett.*, vol. 19, no. 5, pp. 281–283, May 2009.
- [11] M. Jia, Y. Dong, J. Zhang, and X. Luo, "Multilayer composite right/left-hand transmission line with ultra-wideband and miniaturized characteristics," in *IEEE MTT-S Int. Microw. Symp. Dig.*, Denver, CO, USA, Jun. 2022, pp. 356–358.
- [12] R. J. Cameron, "General coupling matrix synthesis methods for Chebyshev filtering functions," *IEEE Trans. Microw. Theory Techn.*, vol. 47, no. 4, pp. 433–442, Apr. 1999.
- [13] R. J. Cameron, "Advanced coupling matrix synthesis techniques for microwave filters," *IEEE Trans. Microw. Theory Techn.*, vol. 51, no. 1, pp. 1–10, Jan. 2003.
- [14] S. Tamiazzo and G. Macchiarella, "Synthesis of cross-coupled filters with frequency-dependent couplings," *IEEE Trans. Microw. Theory Techn.*, vol. 65, no. 3, pp. 775–782, Mar. 2017.
- [15] Y. Zhang, F. Seyfert, S. Amari, M. Olivi, and K.-L. Wu, "General synthesis method for dispersively coupled resonator filters with cascaded topologies," *IEEE Trans. Microw. Theory Techn.*, vol. 69, no. 2, pp. 1378–1393, Feb. 2021.
- [16] L. Szydlowski, N. Leszczynska, and M. Mrozowski, "A linear phase filter in quadruplet topology with frequency-dependent couplings," *IEEE Microw. Wireless Compon. Lett.*, vol. 24, no. 1, pp. 32–34, Jan. 2014.
- [17] F.-J. Chen, L.-S. Wu, L.-F. Qiu, and J.-F. Mao, "A four-way microstrip filtering power divider with frequency-dependent couplings," *IEEE Trans. Microw. Theory Techn.*, vol. 63, no. 10, pp. 3494–3504, Oct. 2015.
- [18] F.-J. Chen, X. Cheng, L. Zhang, Y.-L. Tian, Y. Tang, and X.-J. Deng, "Synthesis and design of lumped-element filters in GaAs technology based on frequency-dependent coupling matrices," *IEEE Trans. Microw. Theory Techn.*, vol. 67, no. 4, pp. 1483–1495, Apr. 2019.
- [19] J.-S. Hong and M. J. Lancaster, *Microstrip Filters for RF/Microwave Applications*. New York, NY, USA: Wiley, 2001.
- [20] R. J. Cameron, C. M. Kudsia, and R. R. Mansour, *Microwave Filters for Communication Systems*, 2nd ed. New York, NY, USA: Wiley, 2018.